Smart soft open point to synergically improve the energy efficiencies of the interconnected electrical railways with the low voltage grids

Tamer Kamel[a], Zhongbei Tian[b,*], Mansoureh Zangiabadi[c], Neal Wade[c], Volker Pickert[c], and Pietro Tricoli[a]

[a] *Department of Electronic, Electrical and Systems Engineering, University of Birmingham, Birmingham, U.K.*
[b] *Department of Electrical Engineering and Electronics, University of Liverpool, Liverpool, U.K*
[c] *School of Engineering, Newcastle University, Newcastle upon Tyne, U.K.*

***Abstract*— This paper presents a novel smart soft open point (sSOP) that interconnects railway electrification system to the local low voltage (LV) distribution grid to provide additional flexibility and controllability for both networks. The proposed sSOP builds on the concept of soft open points, adding an energy storage system and embedding a rail and grid (R +G) energy management system to enable the energy transfer between the two networks at different average power levels. The smartness of the proposed soft open point is realised in the integration of an energy storage system to act as an energy buffer between these two networks of different dynamics. The paper demonstrates that the proposed sSOP improves the braking efficiency of trains and increase the local use of renewable energy through employing an integrated simulation platform between a railway and smart grid simulators that takes into account the trains' timetables as well as the daily variation of the grid loads and renewable energy generation. The results show that an appropriate design and control of the sSOP enables the recuperation of most of the braking energy available from the railway and that energy is enough to mainly supply the local power distribution grid, thereby effectively implementing the concept of smart grids.**

***Index Terms*—Smart soft open point, electrified railway systems, power distribution networks, railway simulator, smart grid simulation.**

* Corresponding author.
E-mail address: zhongbei.tian@liverpool.ac.uk (Zhongbei Tian)

I. INTRODUCTION

After the Paris Agreement [1], the world has committed to move towards a low-carbon economy. The European Union (EU) has set a long-term goal of reducing greenhouse gas (GHG) emissions by 80-95% by 2050 with respect to the levels of 1990 [2]. The primary measure to ensure this transition is the increase of renewable energy sources (RES) and the targeted use of energy storage systems (ESS) to smooth out the power fluctuation of RES and ensure grid stability [3]. The second measure is to electrify more the transport sector by encouraging the electrification of railway lines and the adoption of road electric vehicles (EVs).

The intermittent generation of RES and the deployment of EVs lead to a higher variability of the load of the distribution networks. This variability increases the peak demand of the network but lowers its average utilization, which often require significant investments to reinforce the grid. Electric railways could reduce the peak demand of power distribution networks, because they have available regenerative braking power that can be used with an active energy management of the rail electrification network [4]. For an example, traction power substations (TPSS) occupied with IGBT inverters to feed the braking energy back to the AC grid [5-6] along with providing it with number of ancillary services [7-8]. Additionally, the smart grid approach of electric railways would also improve the efficiency of regenerative braking and enable an efficient management of all the energy sources in the network, including RES [9-11]. In practice, the energy generated by RES and regenerative braking can be either used to meet the network power demand, or stored for shaving power peaks at a later time, thereby achieving significant cost savings by postponing power upgrade programs [12]. Accordingly, integrated solutions are then needed to increase the energy efficiencies of both railway and distribution networks as well as assure the grid stability especially in areas of high penetration of RES and/or high diffusion of EVs charging points. Integration of railways and EVs through park and ride solutions was studied in [13]. Furthermore, authors investigated in [14] the benefits of a DC-link for interconnecting photovoltaic sources, EVs and ESS through a smart hub. Energy management for the railway station is presented in [15] to utilize the regenerative braking energy to supply station loads and emerge it with ESS and PV generation units. Similarly, Flexible TPSS is proposed in [16] to mitigate the problems associated with the electrified railway network negative sequence current, load fluctuation as well improve regenerative braking energy and RES utilization. However, most of this existing literature has not considered the interaction between the railway network and the electrical grid.

Since the railway networks are mainly fed from high-voltage connections, which are not directly connected to local power distribution grids [17]. Therefore, it is more likely that railway networks have fewer constraints than local grids and could be instead be used to support them. The soft open points (SOPs), power electronic devices in place of normally-open points, have been studied to achieve a direct exchange of energy between these independent distribution networks. In these networks, SOPs can control power transfer and optimize network voltage profile by providing fast, dynamic and continues real/ reactive power flow control between feeders [18-19]. A comprehensive review of SOP for distribution applications has been presented in [20], which

summarizes the duty of SOPs and indicates the future research direction on flexibility and robustness. Power flow control mode and supply restoration modes have been proposed to achieve real and reactive power control and enable power supply to isolated loads due to network faults [21]. The SOP operation has been optimized by a non-linear programming algorithm, which considered three objectives including the voltage profile, line balancing and energy losses [22]. To address the global benefit of the SOP, the cost of the SOP has been considered in the operation optimization of a distribution network under extreme typhoon environment [23]. It has been found that implementing only one SOP in the distribution network is both optimal and practical in most simulation cases. Based on the topology SOP can be classified as two-terminal SOP, multi-terminal-SOP. An active distribution network with multiple terminal SOP has been analyzed in [24]. In [24], a multi-time scale robust energy management method has been proposed to decrease system voltage deviation and improve the system robust security under the tolerant cost constraint and renewable energy uncertainty. SOPs can also enhance the system performance and controllability and afford flexible system configuration in both normal and emergencies especially in case of faults [25-26]. Further study on coordinated control for SOP and distributed generator has been investigated in [27], which solves the biconvex problem of voltage regulation by an Alternate Convex Search algorithm. From the literature above, it can be found the SOP operation problems for distribution network has been widely studied. However, there are very few studies on the SOP application in railway and distribution network. The design and performance of SOP for railway applications should be further analyzed.

Trains can regenerate a large amount of energy during electric braking, which can be reused by trains or dissipated in the braking resistances. If the railway can interact with the grid, the energy dissipated can be transferred to support the grid. Accordingly, to enable such features, this paper presents a novel smart SOP (sSOP) that includes an ESS in the dc-link between its converters. ESSs have been already used successfully to reuse regenerated braking energy in urban rail network [28-29]. However, in this new design, the ESS operates as a shared asset between the local distribution grid and the railway network. The ESS is charged frequently for short durations when trains brake, while it releases the energy at lower average power and for longer durations when is needed by the local grid. As the ESS enables power transfer compatibly with the different dynamic characteristics of the two networks, the new sSOP becomes capable to improve the regenerative braking efficiency of the railway network along with reducing constraints on the local LV grid. As a result, the proposed sSOP in this paper is to be considered as a new engineering solution to connect a DC railway network through its DC bus bar to an AC LV distribution network. So, once a nearby braking event in the railway network is indicated, the sSOP will be activated and transfer the available braking power from the railway network to the grid and/or charge the ESS. In view of that, the focus of this application is the active power transfer rather than reactive power exchange and it is mainly different from what SOP application operates in distribution networks which are connected to the AC distribution grid with the same AC voltage level to facilitate the transfer of power between two AC substations or feeders. Consequently, the proposed sSOP aims at interconnecting of these two networks in such controlled way to achieve the

following desired objectives:

- Improve the aggregated braking efficiency of the railway network
- Decrease the energy consumption from the LV grid supplying point
- Increase the local consumption of the RES in the LV grid

Such objectives are greatly realized especially with the synergy between the DC traction system with the LV distribution grids, since the DC traction systems (e.g. metro) have trains of frequent stops during their journeys with shorter distances between their stop stations, contrary to the other traction system like the AC high speed railway systems. As a result, the train braking energy becomes more available to be recuperated and its power level is also more suitable to support the demands of the LV local grid. Therefore, such synergical sSOP application becomes significant alternative for upgrading infrastructure of the LV gird when it comprises with higher demands. In this paper the new proposed sSOP application has been evaluated through an integrated simulation platform developed from two different simulators; railway and smart grid simulators. As a result, the new sSOP is validated with respect to different trains timetables in the railway network as well as the daily variations of the grid loads and renewable energy generation. Besides, since the simulation platform is selected as a main evaluation tool for the new application, the two components of the integrated simulations have to be firstly verified using a real field data to demonstrate their correctness to model the actual physical systems under study.

The paper is organized as follows; section II shows the sSOP architecture interconnecting between an electrified DC railway network and a LV distribution grid along with its control management system. After that, section III describes the mathematical models of the two individual simulators (the railway and smart grid simulators) of the integrated simulation platform, and validate their performance using data from real measurements. Accordingly, the integrated simulation platform becomes capable to include the distinct dynamics of both railway and grid networks. Next, section IV assesses the proposed sSOP at various operational states of the railway network, several load demands of the LV grid and different weather seasons (summer and winter). Finally, Section V draws the conclusions that the proposed sSOP improves the braking efficiency of the railway network and increases the local consumption of the energy generated by RES in the LV grid as well as decreases the energy consumptions of the LV grid from its supplying point.

II. sSOP USED FOR A NEW RAILWAY-GRID INTERCONNECTION

The proposed sSOP interconnecting the DC railway electrification system to the local LV distribution grid is demonstrated in Fig.1. The DC railway networks are fed from HV grid supply points (e.g. 220kV as shown in Fig. 1) through dedicated feeders and step-down transformers in the range of 11-15 kV. This step-downed voltage is then used to supply the DC TPSS as well as the LV AC internal network for the train station loads. Moreover, each TPSS is occupied with transformer/rectifier units to generate

the required DC rail voltage to supply the trains in the network. On the other hand, a local LV distribution grid is also illustrated in Fig.1 feeding residential and commercial loads. It also includes renewables (e.g. solar panels installed on the roofs of residential houses) along with EV charging points at households. The DC rail network typically feeds rail relevant loads (trains and loads at train stations) and attempts to connect it to the LV grid have never been reported. On the other hand, in this presented work and for the first time, an sSOP is used to connect the local LV grid to the DC railway network. The sSOP sits between the DC traction rail and the local grid in which an isolating transformer between the sSOP and the LV grid is existed to ensure galvanic insulation between the railway and LV earth connections. Given that the sSOP is earthed with the earthing of the DC TPSS of the railway network. This earth has then to be isolated from the AC earthing of the distribution grid. Both providers of the distribution and railway network instruct to add such transformer to achieve such isolation for the protection aspect.

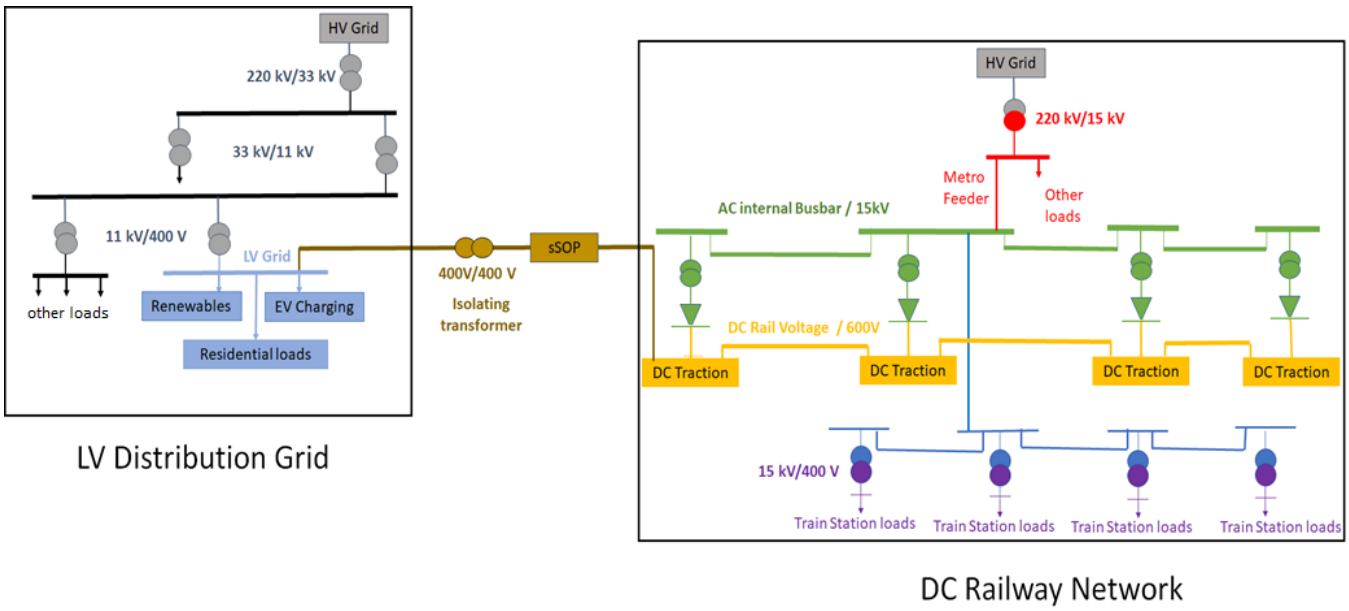

Fig. 1 Architecture for the proposed sSOP interconnection between the DC railway network and local grid

A rail and grid (R+G) control management system is developed to control the sSOP as shown in Fig.2. The R+G management system determines how much power will be harvesting from the rail network during the braking events as well as the power injected to / received from the ESS and grid. The input/output data of the proposed R+G management system are given as follows:

- INPUTs:
  - $P_{SOPrating}$: Power rating of the SOP
  - $P_{B\text{-}Chmax}$, $P_{B\text{-}Dismax}$: Maximum charging and discharging powers respectively of the ESS based on its battery management system (BMS)
  - $P_{Braking|Rail}$: Braking power available from the rail network during braking events.

- $P_{G\text{-}dem}$, $P_{G\text{-}gen}$: Demand and available renewable powers respectively in the grid, $P_{G\text{-}dg}$ is the power difference between them

- OUTPUTs:
  - P_G*: Power Command from the R+G management system for the grid
  - P_B*: Power Command from the R+G management system for the ESS
  - P_R*: Power Command from the R+G management system for the rail network

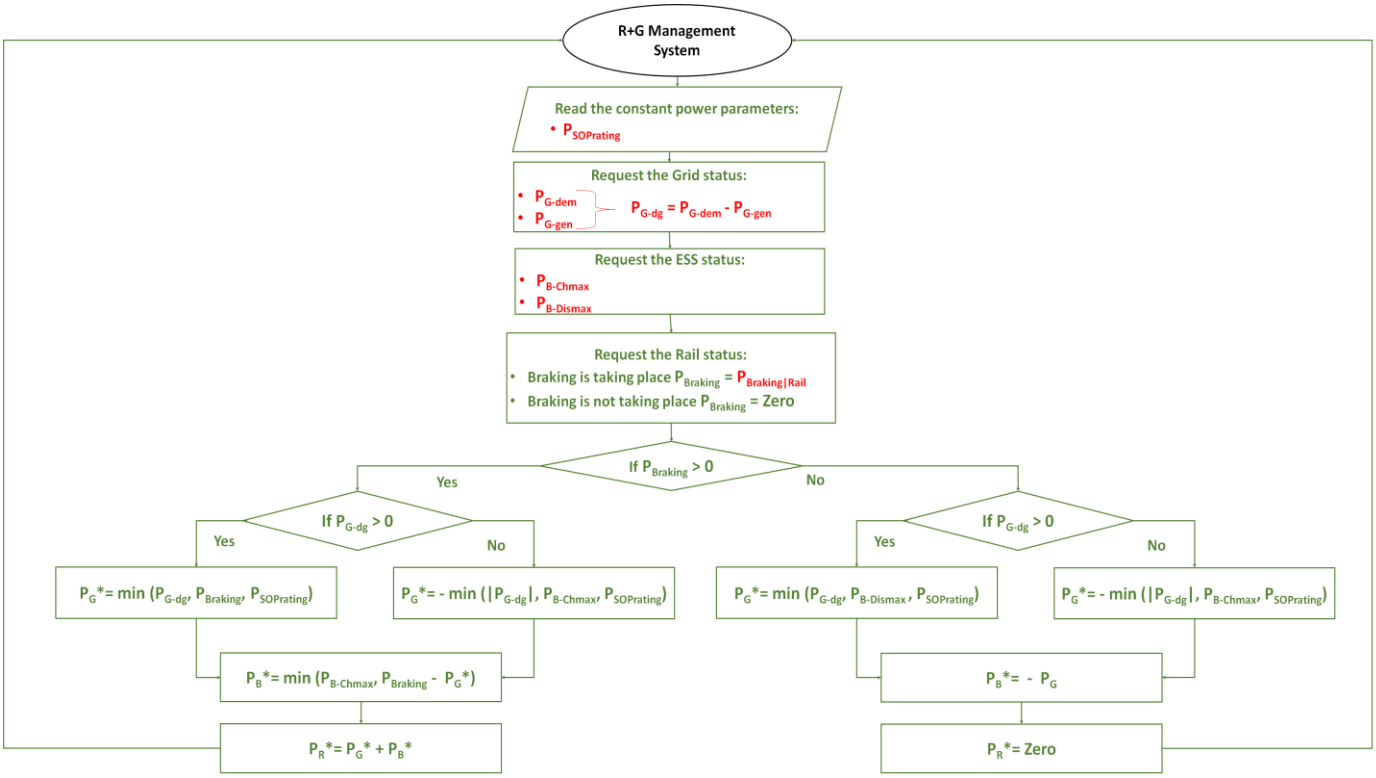

Fig. 2 R+G management system for controlling the sSOP

Accordingly, once the R+G management system reads the statuses of the rail, grid and ESS, it will then determine the power flow between the three individual systems. As a result, during the braking events and the grid is highly loaded ($P_{G\text{-}dg} = [P_{G\text{-}dem} - P_{Ggen}] > 0$), the power injected to the grid becomes as follows:

$$P_G^* = \min\left(P_{G-dg}, P_{Braking}, P_{SOPrating}\right) \quad (1)$$

Where min is the minimum function which selects the lower values from its input parameters. Consequently, P_G* will be employed to either fulfill the exceed in the grid demand ($P_{G\text{-}dg}$) or just transfer the available braking power from rail network to the grid based on which is the lower and meanwhile it won't exceed the SOP power rating ($P_{SOPrating}$) at any condition.

While, if the grid has excess of renewable power (RES) over its demand ($P_{G\text{-}dg} < 0$) whilst the braking event, therefore the received power from the grid is calculated as:

$$P_G^* = -\min\left(|P_{G-dg}|, P_{B-Chmax}, P_{SOPrating}\right) \quad (2)$$

In this case, P_G* is negative value to represent the direction of the power flow from the grid into the SOP. Thus, the P_G* will be utilized to charge the ESS with the minimum from the available excess of power ($|P_{G\text{-}dg}|$) in the grid or maximum charging power of the ESS ($P_{Ch\text{-}max}$), and at the same time, this will be also within $P_{SOPrating}$.

Moreover, during the braking events, the ESS is directed to be charged either from rail or from rail and grid based on grid states, and the charging power of the ESS will also not exceed its $P_{Ch\text{-}max}$ at any condition.

Eventually the commanded power required from the rail (P_R*) will be basically the summation of P_G* and P_B* to balance the system input/output power flow with assuming the system is lossless for simplification.

On the other hand, if there is no braking power available from rail, only the grid and ESS will exchange power depends on the grid states. So, if the grid demand is dominant, the ESS is then discharged into the grid with the minimum of $P_{G\text{-}dg}$, or $P_{Dis\text{-}max}$. while if the RES power exceeds the grid demand, therefore, the ESS is charged from the grid with the minimum of $|P_{G\text{-}dg}|$, or $P_{Ch\text{-}max}$ and keep all the commanded powers within $P_{SOPrating}$ during all conditions.

In this presented management control approach, the supply of the railway traction from ESS and/or LV grid is not considered mainly because both ESS and the LV grid have power ratings substantially smaller than that of the trains demand and, hence, would not be capable of providing an effective contribution. Furthermore, it is unlikely that TPSSs would become overloaded, as they are designed with a reserve capacity of up to three times the nominal ratings within predefined time periods [14]. A framework flowchart for the presented work in this paper is demonstrated in Fig. 3 that is linked to the paper sections

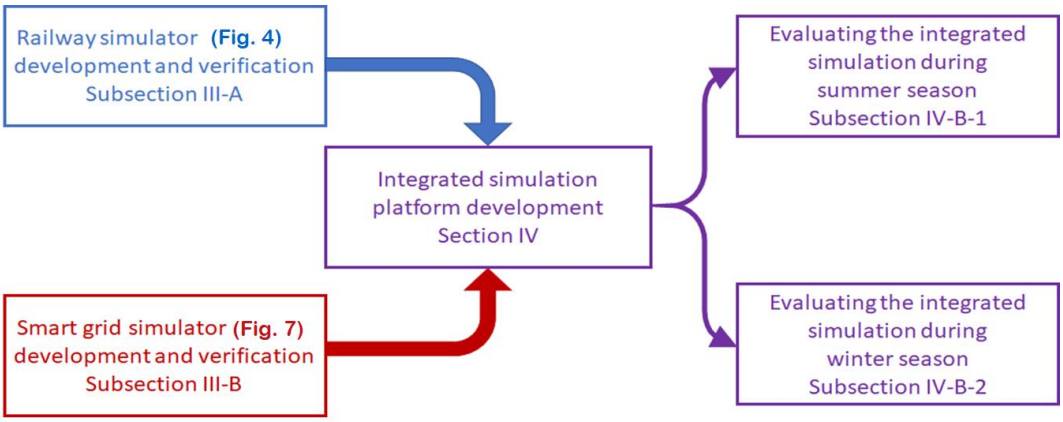

Fig. 3 Framework flowchart for the presented work in the paper

III. CHARACTERISATION OF THE SIMULATION PLATFORM

A. Railway simulator

To understand the train operation and energy consumption, a railway simulator has been developed through MATLAB to simulate a DC metro line [30-32]. The railway simulator combines the train traction simulation and power network simulation. The structure of the railway simulator with main inputs and outputs is shown in Fig.4. Two simulations enable the data transmission with each other to calculate the power performance for the railway network. In the train traction simulation, each train driving characteristics (speed profile, journey time and traction power demand) are calculated by the route profile (distance, speed limit and gradient), train traction characteristics (train mass, tractive effort, traction power, braking power) and driving controls (acceleration, cruising, coasting, and deacceleration). The train speed profile is generated from Newton equations of motion [24]:

$$M_e \frac{dv}{dt} = F - F_g - F_m \tag{3}$$

where M_e is the train effective mass; F is the tractive effort which is determined by driving controls; F_g and F_m are the forces due to the route gradient and train motion. The train mechanical power is the product of traction effort F and train speed v. The electrical power demand can be calculated by:

$$P_{elec} = \frac{Fv}{\eta} + P_{aux} \tag{4}$$

where η is the efficiency of train power chain, and P_{aux} is the train auxiliary power demand.

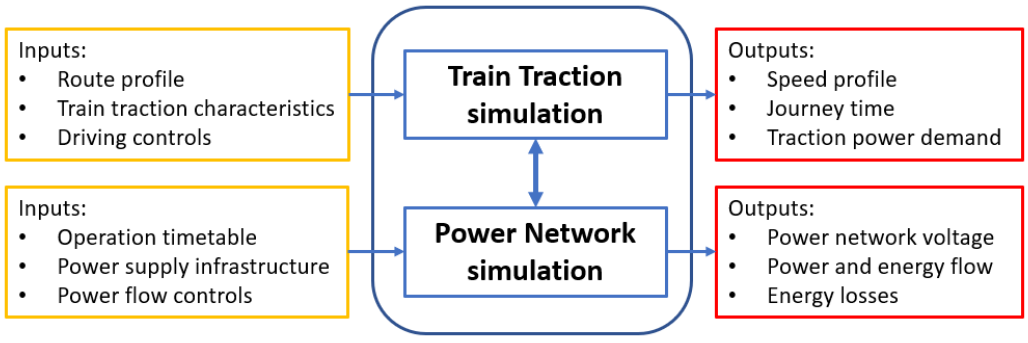

Fig. 4 Railway simulator structure

From the train traction simulation, each train electrical power demand and its location can be obtained. To solve the whole electrical railway network voltage and power follow, the multi-train operation timetable (frequency of trains) is required, which is

used to calculate all train position at time domain. With the train power from train power, position, power supply infrastructure (traction substation position, voltage and rated power capacity) and power flow controls, an equivalent power network can be obtained and solved using iterative power flow algorithms. Finally, the power network simulation will output the voltage and power flow at each network component (train and substation). The energy consumption and losses through the railway network can be analyzed. The substation and railway network voltage will be used in the calculation with the connection of the grid.

The railway simulator has been validated by comparing simulation results with real measurements taken at one of the Metro de Madrid lines, having a total length of 39.4 km, 29 stations and operating at 600 V DC. The measured train speed and power profiles of one train, not shown here for brevity, were used to tune the train model in the simulator. The maximum train traction power of the trains was around 4 MW and the maximum braking power was around 4.8 MW. The DC voltage at the TPSS was measured during the peak hours. The headway time at peak hours is between 4-5 minutes and the simulator emulates this by applying a normally distributed headway time between every two adjacent trains in the same range. The measured and simulated substation DC voltage are compared in boxplots in Fig. 5. It demonstrates that the two distributions have the same average and very close statistical distributions. Specifically, the percentage errors for the median, maximum, and minimum voltage data are 0.25%, 0.13% and 1.25%, respectively. Therefore, the simulated railway power flow results can be assumed as highly close to real results.

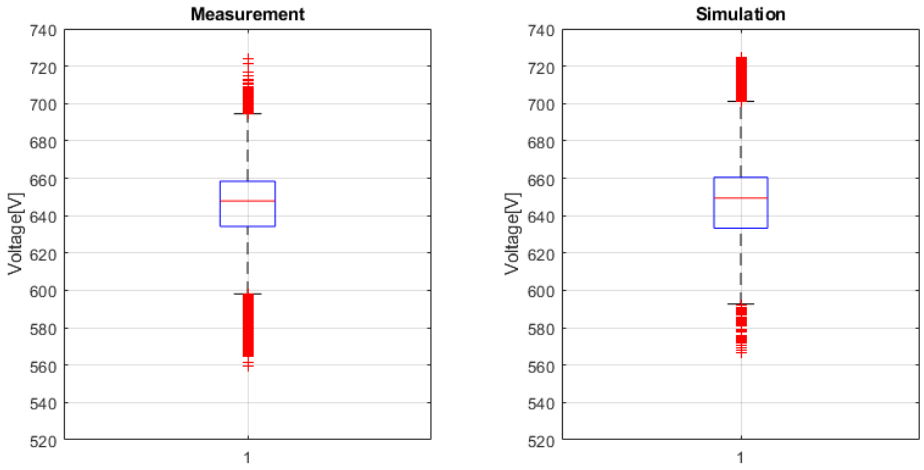

Fig. 5 Boxplot of the measured and simulated substation DC voltage

To demonstrate the multi-train operations where the trains are moving across different stations with timeline, Fig. 7 illustrates the full-day timetable of one of the Madrid Metro lines under study, which operates for 22 hours every day. In this line, there are 36 train cycles every 6.5 minutes, 112 train cycles every 7.5 minutes and the final 8 train cycles every 15 minutes. Fig. 6, gives the train location of every train at different time.

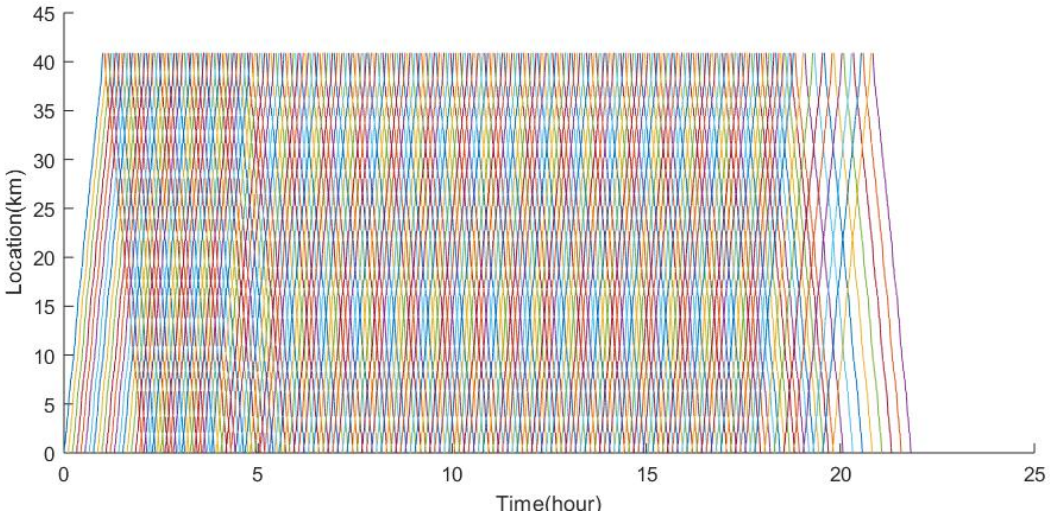

Fig. 6 Timetable of the Metro de Madrid line

B. Smart grid simulator

The smart grid simulator has been implemented in MATLAB using the following load flow equations [33]:

$$P_{Gi} - P_{Di} = \sum_{j=1}^{n} |V_i||V_j||Y_{ij}| \cos\left(\theta_{ij} - \delta_i + \delta_j\right), i = 1, ..., N \tag{5}$$

$$Q_{Gi} - Q_{Di} = -\sum_{j=1}^{n} |V_i||V_j||Y_{ij}| \sin\left(\theta_{ij} - \delta_i + \delta_j\right), i = 1, ..., N \tag{6}$$

where,

V_i, δ_i The magnitude and angle of the voltage at bus i;

V_j, δ_j The magnitude and angle of the voltage at bus j;

P_{Gi} The real power output injected at bus i;

Q_{Gi} The reactive power output injected at bus i;

P_{Di} The real power demand at bus i;

Q_{Di} The reactive power demand at bus i;

Y_{ij} The magnitude of the bus admittance matrix element;

θ_{ij} The angle of the bus admittance matrix element.

The structure of the smart grid simulator is presented in Fig. 7. Accordingly, the buses' voltages and feeders' currents of the simulated grid are estimated through solving (5) and (6) iteratively based on the given network parameters including its single line diagram, cables and transformers specifications to estimated their admittances, and eventually the supply and load power data which could be congregated through smart meters distributed across the simulated grid as has been done in this research.

Fig. 7 Smart grid simulator structure

The performance of the smart grid simulator has been validated comparing the simulation results with measurements taken from a section of the AC internal network of one of the lines of Metro de Madrid (MDM). The configuration of the electrical railway network with connection to the distribution substation operator (DSO) for the studied line is illustrated in Fig. 1. The characteristics of the actual cables of the AC internal network at 15 kV and those used for the metro feeders were used to tune the model.

The designated DSO substation under study is feeding four TPSSs and a number of station loads. Instant real power telemetering data for this DSO was provided by the metro provider (MDM) and gathered for a day every 30 seconds. The boxplot of the power consumption is illustrated in Fig. 8. A simulation study has been carried out using the smart-grid toolbox of MATLAB program to represent one of the TPSS connected to this DSO substation under study, where it is assumed that the measured power consumption is divided equally between the four TPSSs connected to this DSO.

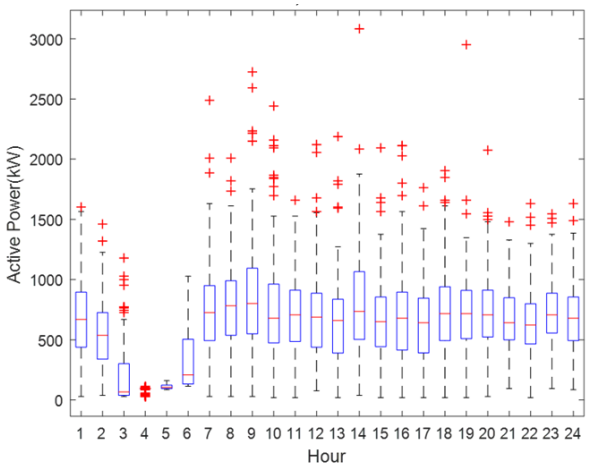

Fig. 8 Boxplot of measured active power of the designated DSO under study

Fig. 9 illustrates the boxplots of the measured and simulated voltage at one of the TPSS and the percentage errors for the median, maximum, and minimum voltage data are 0.06%, 0% and 0.48%, respectively.

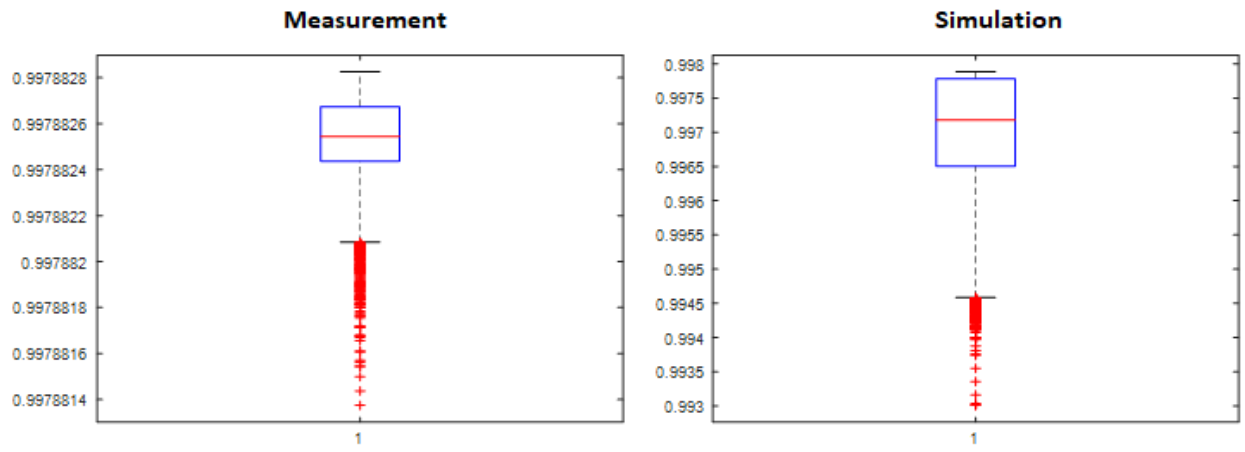

Fig. 9 Boxplot of the measured and simulated TPSS voltage

As a conclusion, both railway and smart grid simulators are separately validated using measurements form real environment and therefore can be used as effective tools to assess the performance of the sSOP.

C. sSOP simulator

The sSOP combines the converters and an ESS. The converters are used to control the power flow among the railways, the grid and ESS. The ESS is used to collect the surplus power from railway regenerative braking and grid renewables, and support the grid when the grid requires power demand. From the railway simulator, the power of substation (P_{sub}) be calculated based on train operation. When $P_{sub} > 0$, the railway network is supplied by the TPSS; when $P_{sub} < 0$, there is available surplus regenerative braking energy which can be used to supply the grid or charge the ESS. From the grid simulator, the power from grid transformer can be obtained (P_{grid}). When $P_{grid} > 0$, the grid requires the power from the grid transformer; when $P_{grid} < 0$, there is surplus renewable energy available from the grid which can be used to charge the ESS.

In the sSOP, when $P_{sub} > 0$, the railway network does not participate the energy flow with ESS and grid. The ESS supplies the grid when $P_{grid} > 0$, and receives power from grid when $P_{grid} < 0$. When $P_{sub} < 0$, the railway substation regenerative power will be used to supply the grid first and the rest of the power will be used to charge the ESS. Therefore, the charging power of the ESS can be calculated by (7). The ESS is charged when $P_{ESS} > 0$, and discharged when $P_{ESS} < 0$.

$$P_{ESS} = \begin{cases} -P_{grid} & when\ P_{sub} > 0 \\ -P_{sub} - P_{grid} & when\ P_{sub} < 0 \end{cases} \tag{7}$$

The state of charge (SoC) is an important parameter to determine the charging/discharging performance of the ESS. The SoC is calculated dynamically by P_{ESS}, the ESS energy capacity (C_{ESS}) and initial SoC as in (6). In this paper, when the SoC is below 0.1, the discharging power will be set to zero. When the SoC is above 0.9, the maximum P_{ESS} will be reduced lineally until to zero when SoC becomes 1.

$$SoC = SoC_{inv} + \frac{\int P_{ESS} dt}{C_{ESS}} \tag{6}$$

IV. Performance Assessment of sSOP for Railway and Distribution Networks

This section shows how the simulation platform is developed by integrating the railway and the smart grid simulators to assess the impact of the proposed sSOP interconnection architecture as demonstrated in Fig. 10, in which the exchange of the power and voltage data is undertaken between the different sections of the two simulators as illustrated in the figure. The integrated simulation platform is carried out for a full day simulation in summer and winter seasons to evaluate the performance of the sSOP at different situations.

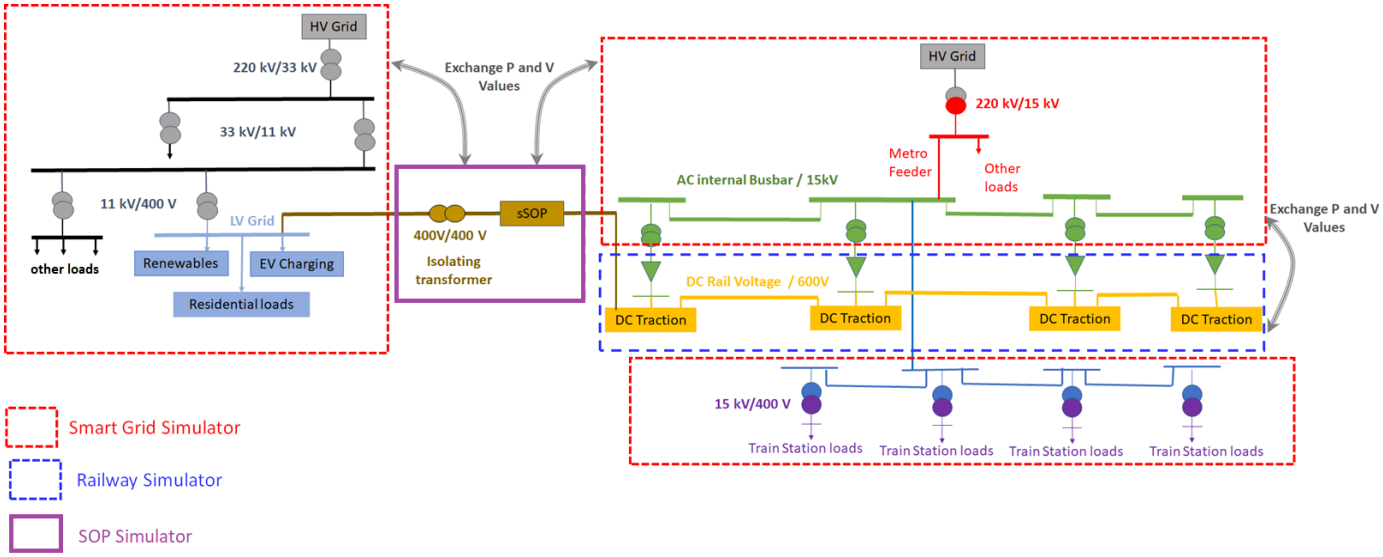

Fig. 10 Structure of the integrated simulation platform

A. LV grid case study

The LV grid under study is a residential LV radial network modeled through real time data [34-35]. The LV network is illustrated in Fig. 11 which a secondary substation (11kV/433V) is feeding 244 households through five feeders. Smart meters collected the data as half-hourly electrical energy consumption in kWh and then the data is converted to average half-hourly power in kW for analysis. The trials were organized into different cells from household's consumptions to solar PV customers and electric vehicle customers. A data set is depicted in Fig. 12 for the summer season to investigate the impact of solar PV generation and EV demand on network.

As seen in the figures, the consumption of a domestic household customer profile follows a unique and predictable pattern throughout the months. The peak demand for a house reaches about 0.95 kW around 18:00 to 21:00 during every month. Moreover, a drop in the load is experienced around morning throughout the measurements. The consumption greatly varies between seasons with peak demand during winter months and low demand during summer months. The measurements of EVs involved customers who owned an electric vehicle and had access to a home charger, were being monitored in 143 homes. The EV demand was averaged across all households, exhibits a significant peak in the evening of about 0.9 kW at around 9:00 pm, broadly equivalent to the house-only consumption peak that occurs at similar time. Like household load, the electric vehicle load drops through the overnight period, but stays around 0.1-0.2 kW during morning and afternoon periods. This behavior in the demand profile is consistent with EVs being used as primary mode of transport, as the owners travel on their electric vehicle during daytime and plug-in it to charge upon returning to home during evening time. However, the peak load during the evening time drops quickly after 10 pm indication that some electric vehicle batteries were fully charged at this point thus reducing the load demand. In a residential area, where EVs are the primary way of transport, domestic charging of EVs could have a major impact on the network, but this will depend on the speed and extent to which EVs are introduced. Whilst this is not yet a problem for network system design and operation, there is a strong case for taking appropriate action to encourage off-peak charging behavior from the outset. The total power consumption of the LV network under study during summer season is plotted in Fig. 13

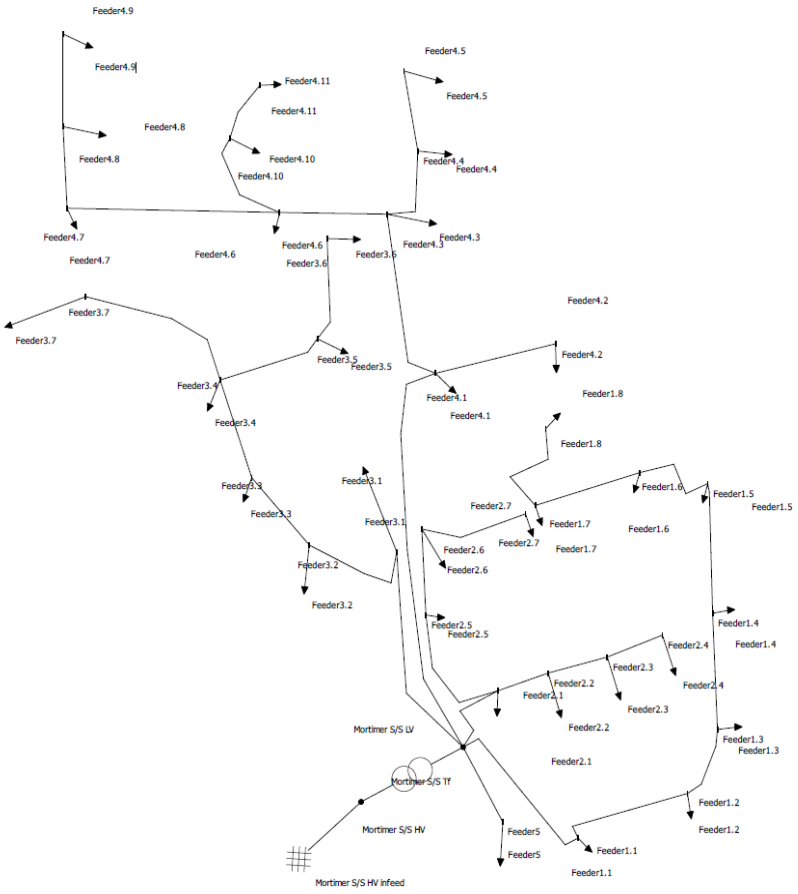

Fig. 11 LV grid network under study

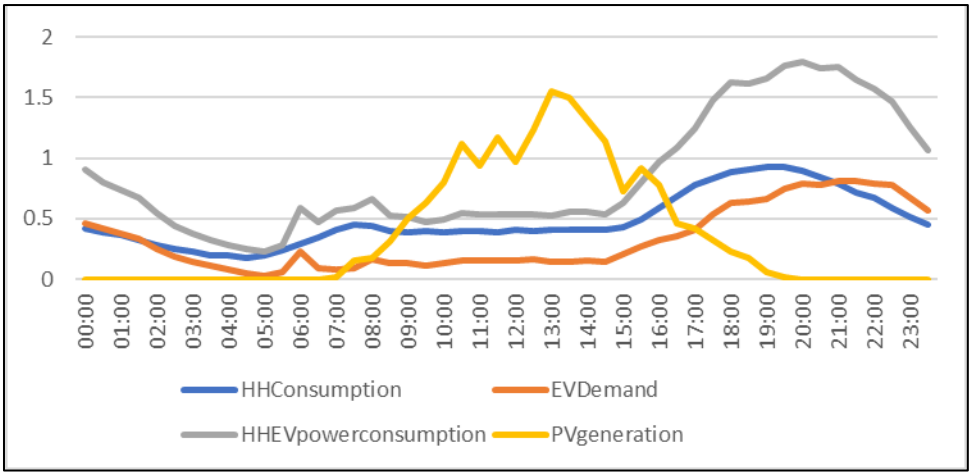

Fig. 12 Mean Monthly during summer season for a domestic household consumption in blue (kW); Solar PV generation in yellow (kW); electric vehicle power demand in orange (kW); combined household and electric vehicle demand (HHEV) in Grey

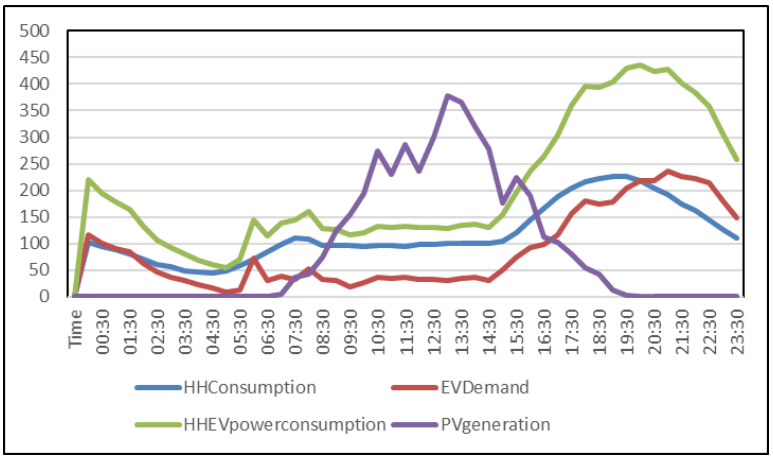

Fig. 13 Total power (kW) for the LV network under study during the summer season.
Blue: domestic household consumption, Purple: solar PV generation ; Red: electric vehicle demand; Green: combined household and electric vehicle demand

B. Simulation results of the sSOP connected across the railway and LV distribution networks

A full-day simulation was conducted incorporating the R+G management system and the sSOP for the interconnected networks of Fig. 10. One of Metro de Madrid lines is used in this study, the parameters are given in Table I. The networks have been simulated without and with the sSOP at one of the TPSS in order to verify the improvement in terms of energy consumption of the LV network and energy efficiency of railway regenerative braking.

TABLE I
Parameters of the electrical railway network

Quantity	Unit	Value
Length of the route	[km]	40.9
Number of stations	-	28
Number of substations	-	11
Substation voltage	[V]	1500
Substation power	[MW]	6.6
Train traction power	[MW]	2.4
Number of train cycles per day	-	156

1) Evaluation of the proposed sSOP during summer

Without the sSOP, the LV network demands 7.80 MWh per day according to Fig. 13 during summer. Besides, the PVs on the LV network generate 2.20 MWh of renewable energy per day. However, not all the renewable energy is consumed within the LV network, as there are hours where supply exceeds the demand and the energy is fed back to the MV network. Specifically, the LV network requires 5.96 MWh per day from the grid transformer and injects 0.29 MWh per day of renewable energy back to the MV grid. This is not ideal, as the energy fed back to the MV network causes extra losses due to the longer distance.

The energy consumption obtained from the simulation for a full-day operation of the railway without and with the new sSOP arrangement is given in Table II. With the new sSOP arrangement, the railway substation energy consumption increase a little bit. This is because some regenerative braking energy is transmitted to the sSOP rather than used by other accelerating trains. It is more efficient to transmit some regenerative braking energy to sSOP rather than to other trains far from the source of regeneration. The total energy transmitted from the railway network to the sSOP is 5.9 MWh per day. Therefore, the regeneration efficiency of the railway network increases from 90.5% to 98.6%, showing that the sSOP increases the regeneration efficiency by 8.1%.

TABLE II
Energy consumption for a whole-day operation with and without the new sSOP arrangement

Quantity	Symbol	Unit	Without sSOP	With sSOP
Energy supplied by all the substations	E_s	[MWh]	103.92	104.56
Energy transmitted from the railway network through sSOP	E_{sSOP}	[MWh]	0	5.9
Energy actually drawn by all the train to complete the journey	$E_{traction}$	[MWh]	134.28	134.28
Energy available from all the train for regenerative braking	$E_{braking}$	[MWh]	70.65	70.65

Actual effective use of regenerated braking energy	E_{regen}	[MWh]	63.95	69.68
Efficiency of regenerative braking, calculated as E_{regen} / $E_{braking}$	η_{regen}	[%]	90.5	98.6

The capacities of sSOP and ESS play significant roles in the energy performance of the integrated network. The capacity of sSOP limits the power transmission capacity among the railway, grid and ESS. In this case study, the capacity of sSOP is the same as the maximum regenerative braking power at the traction substation. Therefore, it allows the maximum regenerative braking power to transmit to ESS and the grid. The ESS capacity is designed to make sure the receptivity of all surplus regenerative braking energy and renewable energy. In this case study, the ESS capacity is designed as 2.5 MWh with the C-rate of 1.2. Therefore, the charging power is 3 MW. This capacity is the minimum capacity which can collect all regenerative and renewable energy every day.

To ensure continuous operations of the system, the state of charge (SoC) of the ESS has to be the same after one-day operation. To achieve this requirement, the LV grid charges the ESS during off-peak hours. Looking at the diagram of Fig. 14, the ESS is charged by the LV grid from 4:00 am to 6:00 am, when there is a limited load demand on the LV network and the railway is not in operation. Moreover, to improve the system efficiency, the ESS capacity and initial SoC have been optimized. From the optimization study it is found that 2.5 MWh of the ESS is the minimum requirement to supply the LV grid during the day for the presented case scenario. Furthermore, if the SoC starts at 0.25 at 0:00 am and the grid transformer charges the ESS with 170 kW from 4:00 am to 6:00 am, the SoC can return to its initial value of 0.25 at the end of day. The SoC profile and power of the ESS during a whole day are shown in Fig. 14 (a) and (b) respectively, in which a positive power means charging the ESS, while the negative power means discharging the ESS.

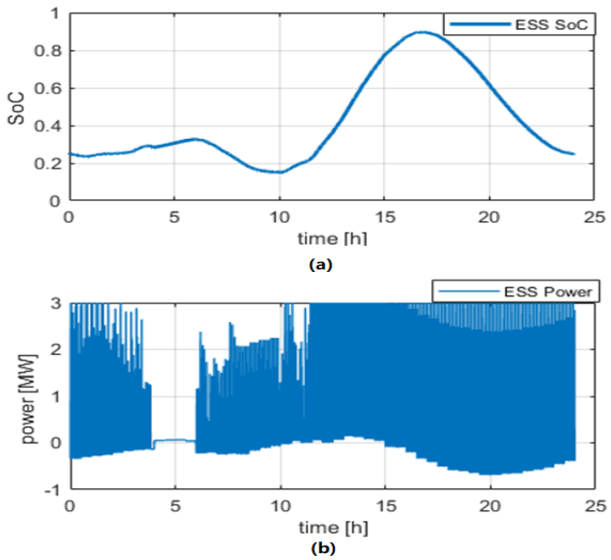

Fig. 14 The daily profiles of (a) the SOC and (b) the power of the ESS for the case under study during the summer season

The main aspects of the ESS profile during the day could be summarized as follows:

- From 0:00am to 4:00am, the SoC does not change a lot since the LV grid demand and rail regenerative power are almost balance each other.
- From 4:00am to 6:00am, The ESS is charging from the grid transformer during this period to keep its final SoC at the end of the day equals to its initial value. Given that there is no train service as well as the grid demand is low at this time.
- From 6:00am to 10:00am, there is some train regenerative power available. However, the SoC of the ESS drops since the LV grid demand is higher than train regenerative power.
- From 10:00am to 16:00pm, SoC starts to increases due to the higher train regenerative power as well as the rise of the RES along with the lower LV grid demand during this period.
- From 16:00pm to 24:00pm, SoC drops due to the higher grid demand again with lower regenerative rail power.

Fig. 14 also shows that the EV charging loads reach around 50% of the total grid demand during the peak time of residential loads. Such profile could represent a challenge for the existing infrastructure and require upgrades of the distribution network. Therefore, the sSOP can be a significant mitigation by supplying the power required by the EV charging from the available braking energy from the railway network. It is worth mentioning that the selection of the initial SOC of 0.25 and a charging power from the grid transformer of 170 kW are case study dependents, in which both parameters can be modified according to the different demand/generated power in the railway and the LV networks per day. Eventually, the power profile of the LV network from grid transformer without and with the inclusion of the new sSOP arrangement are compared in Fig. 15. Fig. 16 as well as Tables II and III show how the new sSOP improves the operation of both railway and LV networks during the summer season. In Table III, it can be found that the energy supplied by the grid transformer is reduced from 7.8MWh to 0.34 MWh with sSOP, avoiding any export of energy to the MV grid. More renewable energy has been used locally within the LV grid, where the percentage of local-consumption of the RES energy in the LV grid increases from 86.5% to 99.7%.

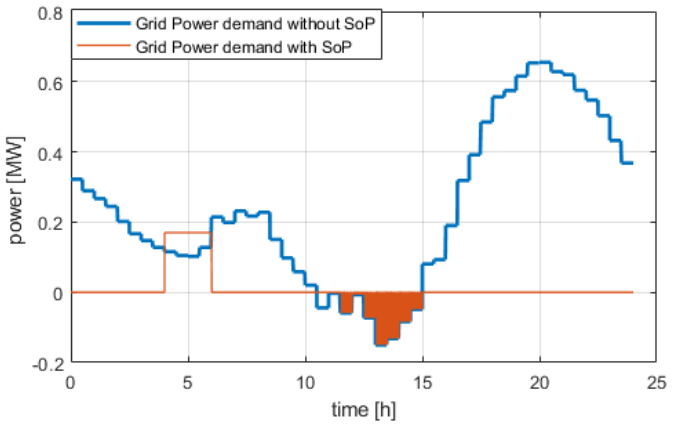

Fig. 15 Daily grid power profiles without and with the new sSOP arrangement during the summer season.

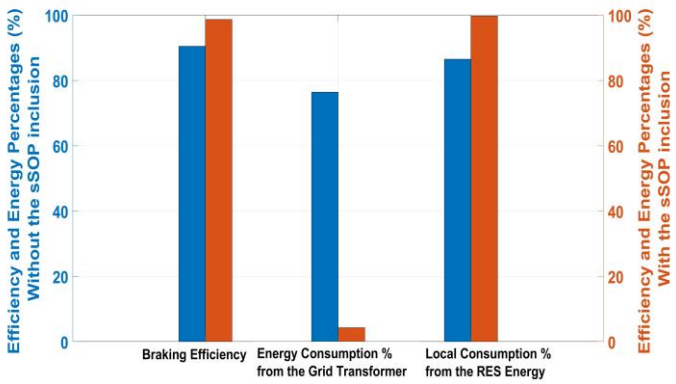

Fig. 16 Efficiency and energy percentages (%) without and with the sSOP inclusion during summer season

TABLE III
Daily energy consumption for the operation with and without the new sSOP arrangement during the summer season

Parameter	Without sSOP	With sSOP
Total grid Demand [MWh]	7.8	7.8
Energy form grid transformer [MWh]	5.96	0.34
Percentage of consumption from grid transformer [%]	76.4	4.4
Total RES Energy [MWh]	2.15	2.15
RES Energy consumed locally in the LV grid [MWh]	1.86	2.14
Percentage of local-consumption of the RES energy in the LV grid [%]	86.5	99.7

2) Evaluation of the proposed sSOP during winter

During winter, the available energy from the PV becomes lower than the summer and is available for shorter time. On the other hand, the average monthly power of the domestic household customer consumption as well as the electric vehicle power demand are mainly the same with respect to their values during the summer season. The captured power data for this case scenario during the winter season is illustrated in Fig. 17.

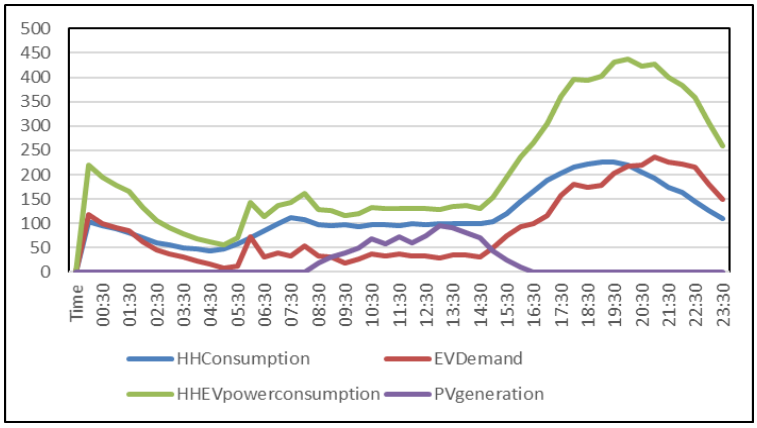

Fig. 17 Total power (kW) for the LV network under study during the the winter season;
Blue: domestic household consumption, Purple: solar PV generation; Red: electric vehicle demand; Green: combined household and electric vehicle demand

During this study test, the ESS capacity is still kept at 2.5 MWh. Since the PV generated energy is lower in winter, more energy is required from ESS to supply the grid during the day. Therefore, the charging period of the ESS from the LV grid is modified during winter from 2am to 6am with a power of 540 kW. Besides, the initial SOC is re-set to be at 0.18, but the SoC is still returned to its initial value at the end of day. The SoC profile and ESS power profile during a day in winter are shown in Fig. 18.

The power profile of the LV network from the grid transformer without and with sSOP are compared in Fig. 19 for winter. With the sSOP, the grid transformer supports 2.16 MWh to charge the ESS in this case study. The power of the grid transformer reduces several times between 2:00 to 4:00 am since there are still some trains in operation and, hence, the ESS is entirely charged by the regenerated power from the braking. Fig. 20 and Table IV show the improvements that have been achieved by the sSOP for both railway and LV networks.

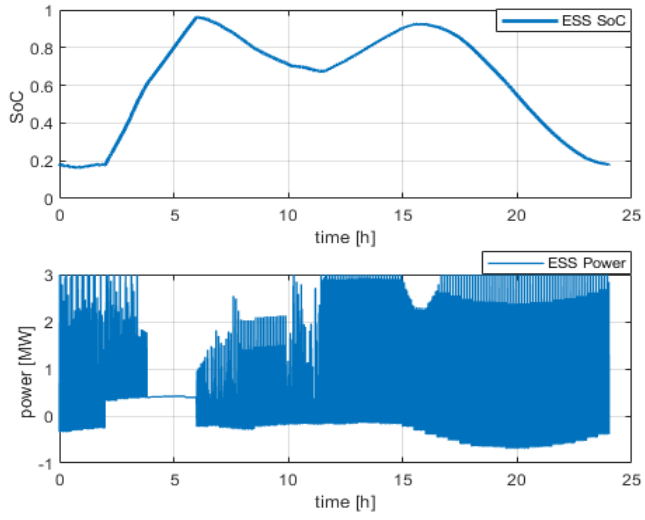

Fig. 18 The daily profiles of (a) the SOC and (b) the power of the ESS for the case under study during the winter season

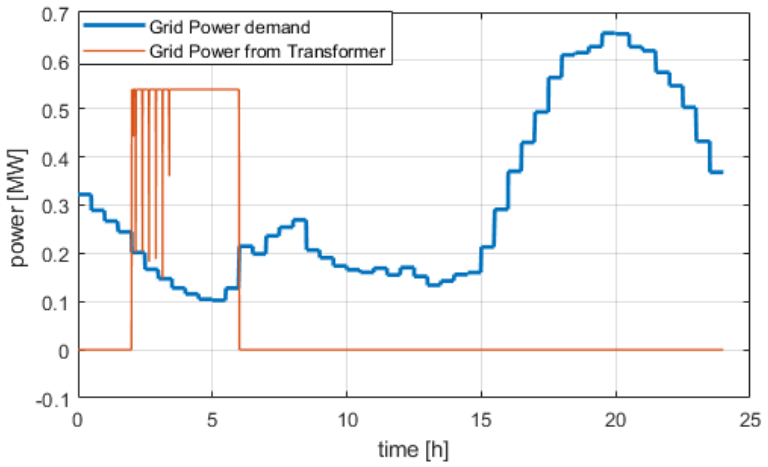

Fig. 19 Daily grid power profiles without and with the new sSOP arrangement during the winter season.

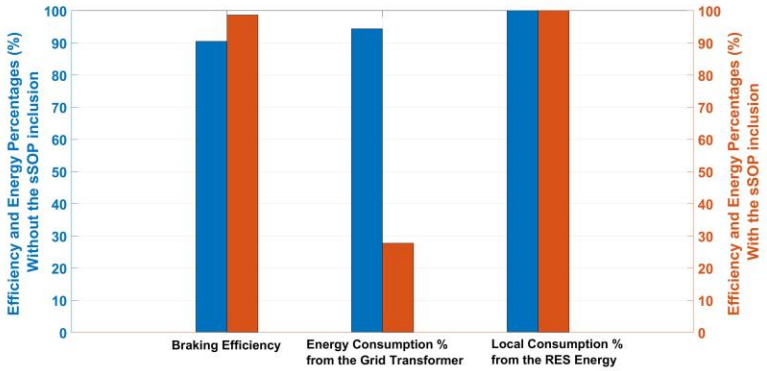

Fig. 20 Efficiency and energy percentages (%) without and with the sSOP inclusion during winter season

TABLE IV
Daily energy consumption for the operation with and without the new sSOP arrangement during winter season

Parameter	Without sSOP	With sSOP
Total grid Demand [MWh]	7.8	7.8
Energy from grid transformer [MWh]	7.36	2.16
Percentage of consumption from grid transformer [%]	94.4	27.7
Total RES Energy [MWh]	0.44	0.44
RES Energy consumed locally in the LV grid [MWh]	0.44	0.44
Percentage of local-consumption of the RES energy in the LV grid [%]	100	100

V. Conclusion

This paper presents for the first time a method how to interconnect a railway electrification network with a local LV distribution grid. A SOP associated with ESS is used to connect between the two networks and a R+G energy management system is developed to control the energy transfer between rail and LV grid. The combination of such SOP and ESS with the R+G management system turns the SOP into a smart SOP (sSOP) which enables the electrical energy available from regenerative braking of trains to be exported to the local LV grid by using the ESS as a shared buffer between them. Therefore, the braking energy of the train, that is characterized by high-power and short duration, could be efficiently transferred to the LV grid that requires lower power but at longer duration. The sSOP has been assessed through an integrated simulation platform in MATLAB program combining a railway simulator and a smart grid simulator for a case study of a DC metro network interconnected to a LV grid feeding residential loads along with some RES power available from the solar panels installed on the roofs of the residential houses.

The proposed sSOP aims at interconnecting rail and grid network which possess different dynamics to make the best use of the available energy on both networks by accomplishing the following targets:

- Improve the aggregated braking efficiency of the railway network
- Decrease the energy consumption from the LV grid supplying point
- Increase the local consumption of the RES in the LV grid

The simulation results show that, during the summer season, the aggregated braking efficiency of the railway network is improved by 8.1% while the energy consumption from the grid transformer is reduced by 94%. Besides, the local consumption of RES is increased by 13.2%. On the other hand, during the winter season, the aggregated braking efficiency keeps the same improvement of 8.1%, while the energy consumption from the grid transformer is reduced by 70%. The local consumption of RES remains the same, as the power generated by local solar panels was already totally utilized in the LV grid without the sSOP. For both cases, the results clearly show the potential of the sSOP to support the LV grid, especially for the peak evening time. This would be particularly important for the wide diffusion of the EVs, charging is expected to occur at the same time of the evening peak and the additional load for charging would cause significant constraints on the grid and likely require reinforcements or upgrading the grid infrastructure.

VI. Acknowledgment

This work has been developed as a part of the project E-LOBSTER. This project has received funding from the European Union's Horizon 2020 research and innovation programme under grant agreement No 774392.

VII. REFERENCES

[1] The Paris Agreement, 2020 United Nations Framework Convention on Climate Change, [Online]. Available: https://unfccc.int/process-and-meetings/the-paris-agreement/the-paris-agreement

[2] Regulation (EC) No 1099/2008 of the European Parliament and of the Council of 22 October 2008 on energy statistics, [Online]. Available: https://ec.europa.eu/eurostat/web/energy/legislation

[3] C. Cheron, M. Walter, J. Sandor, and E. Wiebe, "ERRAC Roadmap. Towards 2030: energy, noise and vibration European railway roadmaps". Procedia-Social and Behavioral Sciences, 2012, no. 48, pp.2221-2229.

[4] C. Chéron, M. Walter, J. Sandor, E. Wiebe, "ERRAC – European railway energy roadmap: towards 2030, In: 9th World Congress on Railway Research" WCRR 2011, Lille, France, 2011.

[5] H. Douglas, C. Roberts, S. Hillmansen, F. Schmid, "An assessment of available measures to reduce traction energy use in railway networks," Energy Convers Manage Vo. 106, pp 1149-1165, 2015.

[6] A. González-Gil, R. Palacin, P. Batty, "Sustainable urban rail systems: Strategies and technologies for optimal management of regenerative braking energy," Energy Convers Manage, vol. 75, pp.374-388, 2013.

[7] A. Bitoleanu, M. Popescu, CV. Suru, "Theoretical and experimental evaluation of the indirect current control in active filtering and regeneration systems," In: 2017 International Conference on Optimization of Electrical and Electronic Equipment (OPTIM) & 2017 Intl Aegean Conference on Electrical Machines and Power Electronics (ACEMP), 2017, pp. 759–764.

[8] M. Popescu, A. Bitoleanu, M. Dobriceanu, "FBD-based control in active DC-traction substations," In: 2016 International Conference on Applied and Theoretical Electricity (ICATE), 2016, pp. 1–6.

[9] Salvatore D'Arco, Luigi Piegari, and Pietro Tricoli. "Comparative Analysis of Topologies to Integrate Photovoltaic Sources in the Feeder Stations of AC Railways." IEEE transactions on transportation electrification, vol. 4, no.4, pp.951-960, 2018.

[10] E. P. de la Fuente, S. K. Mazumder, and I. G. Franco, "Railway electrical smart grids: An introduction to next-generation railway power systems and their operation," IEEE Electrific. Mag., vol. 2, no. 3, pp. 49–55, Sep. 2014.

[11] X. Shen, H. Wei, and L. Wei, "Study of trackside photovoltaic power integration into the traction power system of suburban elevated urban rail transit line," Applied Energy, vol. 260, pp. 114177, 2020.

[12] A.E. Díez, I.C. Díez, J.A. Lopera, A. Bohorquez, E. Velandia, A. Albarracin, M. Restrepo, Trolleybuses in smart grids as effective strategy to reduce greenhouse emissions, In: IEEE International Electric Vehicle Conference – IEVC 2012, Greenville, USA; 2012.

[13] C. Webb, M. Zangiabadi, R. Palacin, N. Wade, 'Integration of Electric Vehicles and Rail through Park-and-Ride Infrastructure', Prco. 25th International Conference and Exhibition on Electricity Distribution (CIRED2019), Madrid, Spain, 2019, no.(1647), pp.1-5

[14] N Wade, C Mullen, M Zangiabadi, M Feeney, N Jakeman, 'Smart-Hubs- DC interconnection and management of PV, EV and ESS', Prco. 25th International Conference and Exhibition on Electricity Distribution (CIRED2019), Madrid, Spain, 2019, no.(1334), pp.1-5.

[15] İ. Şengör, H. C. Kılıçkıran, H. Akdemir, B. Kekezoglu, O. Erdinç, and J. P. S. Catalão, "Energy Management of a Smart Railway Station Considering Regenerative Braking and Stochastic Behaviour of ESS and PV Generation," IEEE Transactions on Sustainable Energy, vol. 9, no. 3, pp. 1041-1050, 2018.

[16] Y. Ying, Q. Liu, M. Wu, and Y. Zhai, "The Flexible Smart Traction Power Supply System and Its Hierarchical Energy Management Strategy," IEEE Access, vol. 9, pp. 64127-64141, 2021.

[17] Hill, R., "Electric railway traction, Part 3 Traction power supplies", Power Engineering Journal, 1994, pp. 275-286

[18] W. Cao, J. Wu, N. Jenkins, et al, "Benefits analysis of Soft Open Points for electrical distribution network", Applied Energy, 2016, no.165, pp. 36-47.

[19] H. Ji, C. Wang, et al, "SOP-based islanding partition method of active distribution networks considering characteristics of DG, energy storage system and load", Energy, 2018, vol.155, pp.312-325.

[20] H.S.Faud, H. Hafezi, K. Kauhaniemi, A.H. Laaksonen, "Soft Open Point in Distribution Networks", IEEE Access, 2020, vol.8, 210550-210565.

[21] W. Cao, J. Wu, N. Jenkins, et al, "Operating principle of Soft Open Points for electrical distribution network operation", Applied Energy, 2016, no.164, pp. 245-257.

[22] C. Long, J. Wu, L. Thomas, et al, "Optimal operation of soft open points in medium voltage electrical distribution networks with distributed generation", Applied Energy, 2016, no. 184, pp.427-437

[23] J. Zhang, A. Foley, and S. Wang, "Optimal planning of a soft open point in a distribution network subject to typhoons," International Journal of Electrical Power & Energy Systems, vol. 129, pp. 106839, 2021.

[24] F. Sun, M. Yu, Q. Wu, and W. Wei, "A multi-time scale energy management method for active distribution networks with multiple terminal soft open point," International Journal of Electrical Power & Energy Systems, vol. 128, pp. 106767, 2021.

[25] J. Wang, N. Zhou, C. Y. Chung, and Q. Wang, "Coordinated Planning of Converter-Based DG Units and Soft Open Points Incorporating Active Management in Unbalanced Distribution Networks," IEEE Trans. Sustain. Energy, pp. 1-1, 2019.

[26] M.B.Shafik, et al, "Adequate Adequate Topology for Efficient Energy Resources Utilization of Active Distribution Networks Equipped With Soft Open Points", IEEE Access, 2019, vol.7, pp.99003-99016.

[27] Y. Zheng, Y. Song, and D. J. Hill, “A general coordinated voltage regulation method in distribution networks with soft open points,” International Journal of Electrical Power & Energy Systems, vol. 116, pp. 105571, 2020.

[28] D. Iannuzzi, F. Ciccarelli, D. Lauria, "Stationary ultracapacitors storage device for improving energy saving and voltage profile of light transportation," Transportation Research Part C: Emerging Technologies 2012; 21(4), pp.321-37.

[29] González-Gil A, Palacin R, Batty P, Powell JP. “A systems approach to reduce urban rail energy consumption”. Energy Conversion and Management 2014, 80, 509-524.

[30] Z. Tian, N. Zhao, S. Hillmansen, C. Roberts, T. Dowens, and C. Kerr, "SmartDrive: Traction Energy Optimization and Applications in Rail Systems," IEEE Transactions on Intelligent Transportation Systems (Early Access), DOI: 10.1109/TITS.2019.2897279, 2019.

[31] Z. Tian, T. Kamel and P. Tricoli, "A study to design the locations of reversible traction substations for minimizing power losses of DC railways," 2019 21st European Conference on Power Electronics and Applications (EPE '19 ECCE Europe), Genova, Italy, 2019, pp.1-9

[32] G. Zhang, Z. Tian, P. Tricoli, S. Hillmansen, Y. Wang and Z. Liu, "Inverter Operating Characteristics Optimization for DC Traction Power Supply Systems," in IEEE Transactions on Vehicular Technology, vol. 68, no. 4, pp. 3400-3410, April 2019

[33] R. D. Zimmerman, C.E. Murillo-Sanchez, MATPOWER software. Available: http://matpower.org

[34] Gareth Powells, Harriet Bulkeley, Sandra Bell, Ellis Judson, “Peak electricity demand and the flexibility of everyday life”, Geoforum, Volume 55, 2014, Pages 43-52.

[35] Customer-Led Network Revolution, 2021, http://www.networkrevolution.co.uk/